Egyptian Journal of Pure and Applied Science

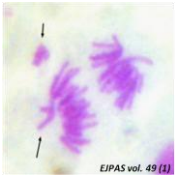

Mixed CdS/TiO_2 Nano Materials for UV-VIS Synergistic Photodegradation of some Heterocyclic Nitrogenous Bases

Mona K. Farhan[1], Mohamed S. Fouda[1], Mustafa H. El-Noss[1], S. A. El-Sadany[1,2], Saeed El-Sayed[1,2], Randa Salah-El-Deen[1], Doaa A. Hamouda[1], Esam Bakier[1], Mohamed S. Attia[1*]

[1]*Nanophotochemistry and Solarchemistry Lab, Department of Chemistry, Faculty of Science, Ain Shams University, Abbassia, 11566, Cairo. Egypt,*

[2]*Forgery and Counterfeiting Department, Forensic Medicine Authority, Ministry of Justice, Cairo, Egypt*

A R T I C L E I N F O

Article history:
Received 13 December 2010
Accepted 29 December 2010

Keywords:
Photocatalytic degradation;
Heterocyclic nitrogenous bases;
UV-Vis light;
Nano material;
Photo liability.

A B S T R A C T

Heterocyclic nitrogenous bases such as Acridine Orange (Dye 1) and its derivative 1,3-dihydroxy-10-carboxylic Acridine (Dye 2) are of immense concern from point view of environment since they are known for their toxic and carcinogenic properties as well as lethal effect on natural biogenic environment. There is a need to control these compounds from getting discharged into the environment. This paper addresses the photocatalytic treatment for the efficient removal to achieve a treated effluent quality fit for disposal without causing any damage to the environment. Efficient mixed CdS/TiO_2 catalyst was produced by simple combustion method at 200 °C. The TiO_2/CdS nano material compared with pure TiO_2 (P25) has the best photocatalytic degradation activity of the heterocyclic nitrogenous bases tested due to its larger abilities of adsorption and light absorbance. UV-Vis light photons synergistically contribute in accelerated reactive species generation, which aggressively attack the pollutants leading to efficient removal. However, dye structure plays a significant role in its photo liability. The results reveal more photo liability of (Dye 1) due to the easy cleavage of the bulky $N(CH_3)_2$ groups, which significantly depress electron delocalization leading to bond weakening.

Introduction

Acridine Orange (AO; Dye 1) and some of its derivatives are heterocyclic dyes containing nitrogen atoms, which are widely used in the field of printing and dyeing, leather, printing ink and lithography[1-3] these dyes are also used extensively in biological staining. Toxicological investigations indicate that aminoacridine has mutagenic potential[4] such type of compounds is a serious pollutant in wastewater and difficult to treat by common removal methods such as coagulation and biodegradation, but few studies on its treatment have appeared. The release of wastewater containing these dyes poses a dramatic source of water pollution, eutrophication and perturbation of aquatic life[5-6]. Therefore, an efficient method of treating wastewater-containing AO and derivatives is highly desirable. Furthermore, molecular structure-photodegaradation correlation will be studied.

In the course of attempts to produce nano catalysts with improved properties[7-11], a mixed catalyst was prepared in aiming to improve photocatalytic properties of TiO_2. CdS/TiO_2 composites were prepared by a method not yet described in the literature, which is, the combustion formation and simultaneous thermal decomposition of cadmium thiourea impregnated on TiO_2 surface. The catalyst will be characterized by its absorption spectrum, XRD and TEM measurements. The photocatalytic degradation of Acridine orange hydrochloride hydrate (Dye 1) and its derivative 1,3-Dihydroxy-9-Acridine carboxylic acid (Dye 2) will be investigated in aqueous suspension of mixed CdS/TiO_2 and irradiated by light covering UV-Visible or UV or visible regions.

Experimental and Methods:

Reagents

All reagents and dyes were of pure or analytical grade (Aldrich and Fluka) and were used as received. The solutions were prepared with pure distilled water. TiO_2 Degussa P-25 was used for the preparation of the TiO_2 nanocomposite materials.

* Corresponding author.
E-mail address: mohamed_sam@yahoo.com.

Materials synthesis:

Nano CdS-TiO_2 composite was prepared by Cadmium Acetate-thiourea complex thermolysis route at 200^0C in presence of TiO_2 P25.

Instrumentation

UV-VIS Measurements:

The optical absorption of the dye solution was measured in the range of 220 –750 nm with a double beam Helios spectrophotometer using distilled water in the reference beam.

XRD Measurements

Identification of the crystal phases precipitating due to the course of crystallization of the powdered samples was conducted by X-ray diffraction analysis. The X-ray diffraction patterns were obtained by using Bruker- AXS D8 Advance, with Ni filtered Cu-Ka radiation. The reference data for the interpretation of the X-ray diffraction patterns were obtained according to the Joint Committee on Powder Diffraction Standards (JCPDS) files. CMRDI

TEM Measurements

The JEOL JEM-1230 available at NRC, Dokki, Cairo was used. JEOL JEM-1230 is a high performance, high contrast, 40-120 kV transmission electron microscope with excellent imaging capabilities. Imaging modes include bright and dark field and electron diffraction. The electron gun is a standard tungsten filament. The instrument is capable of magnifications from 50x to 600,000x and resolution at 120 kV is 0.2 nm.

Photoillumination Setup: A homemade photoreactor (PHOCAT 120) was used.

PHOCAT 120 is designed for Top and Side irradiation. Different wavelength ranges in UV and visible spectrum regions are provided by black, blue or white broadband fluorescent lamps (120 Watts). Irradiation chamber is 43 cm wide, 32 cm deep, and 24 cm high, which is provided with constant speed magnetic stirrer, several switch that, allow the choice of lamps, fan and magnetic stirrer. The chamber is provided with water-cooled capability. The efficient airflow design stabilizes the temperature about 3 degrees Celsius above room temperature.

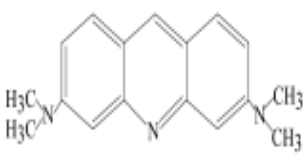

Acridine orange hydrochloride hydrate

[Dye 1]

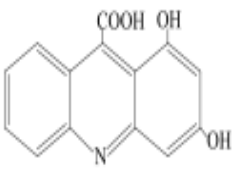

1,3-Dihydroxy-9-Acridine carboxylic acid

[Dye 2]

Results and discussion

Catalyst characterization

UV-VIS absorption spectra of TiO_2 and mixed CdS/TiO_2 reveal the red shift, which should result in enhancing visible light response of the mixed CdS/TiO_2 catalyst, Fig. 1.

XRD spectra

Figure 2 shows the XRD pattern of TiO_2 compared with combined CdS/TiO_2. The average size of crystallites was calculated to be about 15 nm according to scherrer's equation. CdS/TiO_2 composites are mainly composed of anatase phase and small percentage of rutile and CdS cubic phases appeared at 2θ = 26.58, 44.18, 52.18. The presence of CdS results in decreasing the particle size of TiO_2.

TEM measurements

Figure 3 shows a TEM images of pure CdS (cubic and hexagonal mixed phased), TiO2 (P25) and CdS-TiO_2 morphology [average particle diameter of ca. 17.5, 23, 15 nm, respectively]

Photocatalytic degradation of Dyes 1 and 2

Photocatalytic activity

A blank experiment in the absence of the photocatalyst under UV-Vis irradiation showed remarkable photostability. Fig. 4.

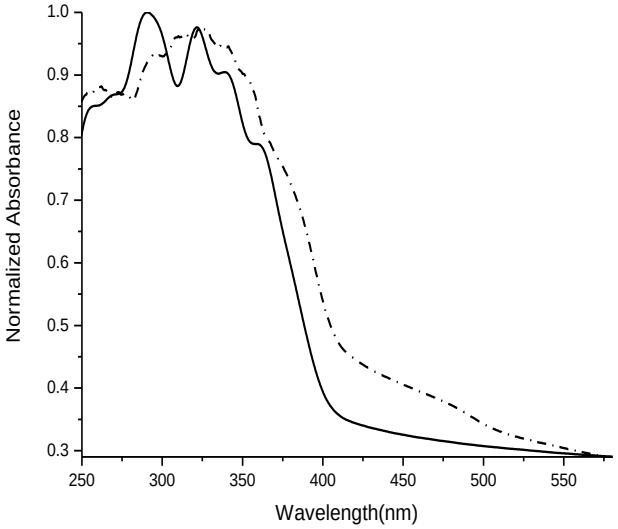

Fig. 1: Normalized absorbance spectrum of TiO_2 degauss and it's doped with nano 2% wt of CdS. (solid line TiO_2 and dash line CdS/TiO_2).

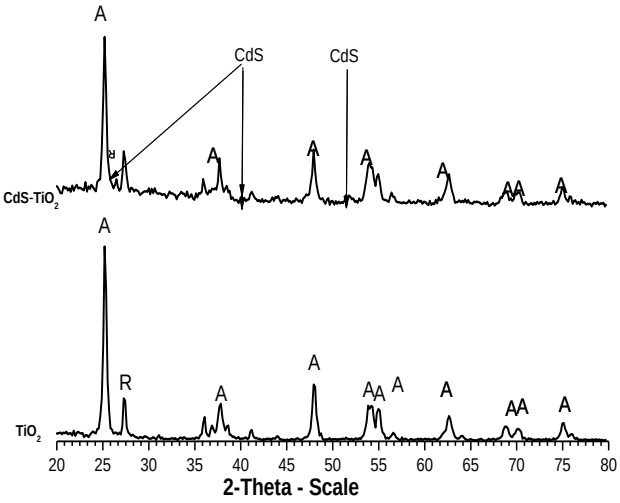

Fig. 2: XRD of TiO_2 and CdS/TiO_2.

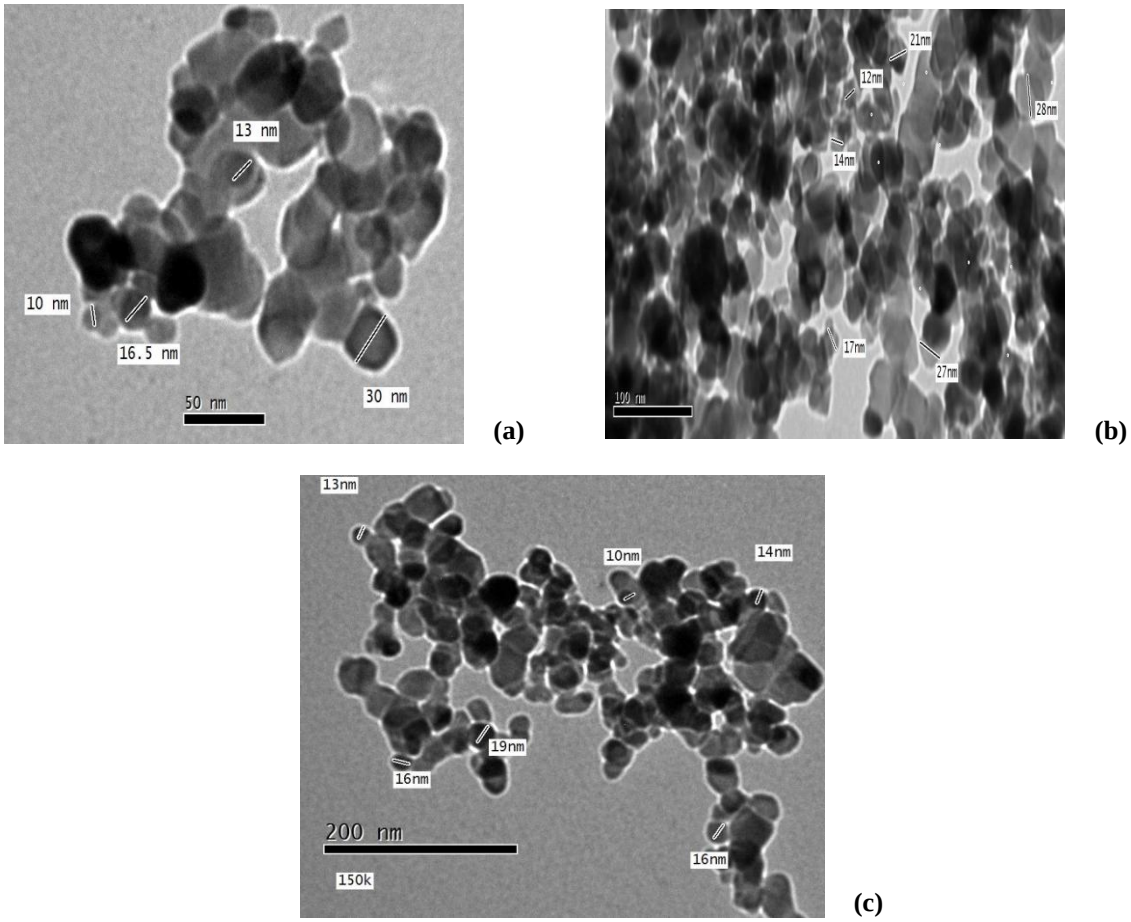

Fig 3: TEM images of pure CdS (cubic and hexagonal mixed phased), TiO2 (P25) and CdS-TiO_2 morphology [average particle diameter of ca. 17.5, 23, 15 nm, respectively].

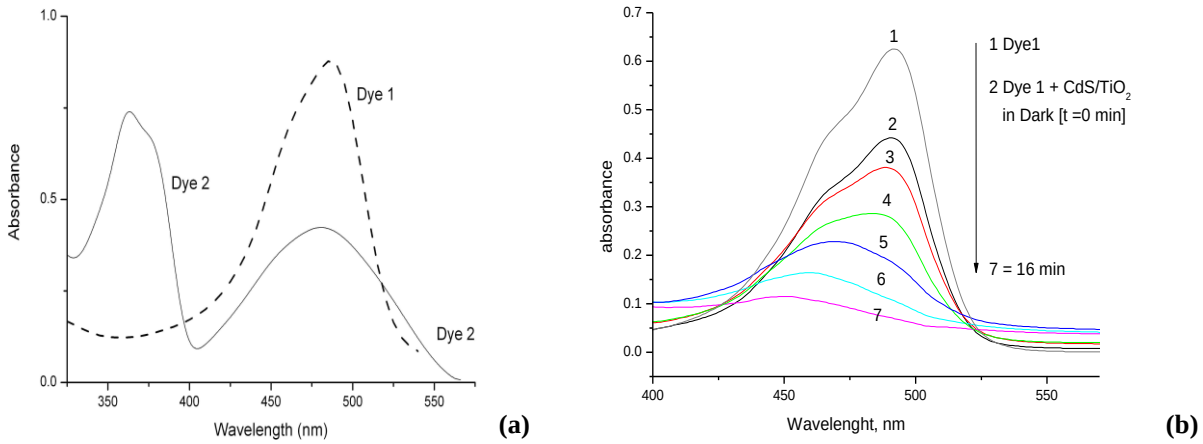

Fig 4: The visible- absorption spectra of aqueous solutions of Dyes 1 and 2 (a) Effect of catalyst in dark (line 2) showing significant adsorption of the dye on the catalyst and effect of catalyst/UV-VIS at different time intervals (lines 3 – 7)(b)

Kinetic studies

These spectra were obtained as a function of time and analyzed to calculate the dye degradation percentage [degradation efficiency] as indicated in Eq. (1) and the speed of the reaction for each case.

$$\text{Degradation\%} = [1-A_t/A_0] \times 100 \quad (1)$$

$A_{(t)}$ is the absorbance after a time t and A_0 is the dye initial absorbance.

The kinetics of the reaction was obtained for all the samples by plotting $-\ln(A_t/A_0)$ as a function of time Eq. (2).

$$-\ln(A_t/A_0) = kt \quad (2)$$

The rate of reaction for the different samples is given in Table 1. Eq. (2) is valid for first order kinetics as it is explained by the well-known Langmuir–Hinshelwood model for low dye concentrations[12]. Table 2 shows the band positions of the studied semi-conductor photocatalysts in aqueous solution. Cadmium sulphide is one of the very well known semiconductors. It has a narrow band gap of 2.4 eV. Kinetic investigations show that the CdS/TiO_2 system is effective in the case of the photodegradation of Dye 1 and 2 in water. The data obtained of the rate constant and degradation% are shown in table 3**.**

Table 1: The decolonization rates and efficiency (D%) of Dyes 1 and 2 using suspended CdS/TiO_2 Degussa P25. [Dye 1]=2.0x10^{-5}M, [Dye 2] = 2x10^{-4} M, pH=7 (aqueous solution). ($\lambda_{Analytical}$=480nm). Optimum load weight of the catalysts was 1gl^{-1}.

Dye	Catalyst/light	Rate/min^{-1}	D%
1	TiO_2/ UV-Vis	0.14	87.0
	CdS/TiO_2/ UV-Vis	0.23	100
	CdS/TiO_2/ Vis	0.07	17.0
2	TiO_2/ UV-Vis	0.05	51.5
	CdS/TiO_2/ UV-Vis	0.07	65.0
	CdS/TiO_2/ Vis	0.05	5.0

Error limits = ±0.02

Table 2: Band positions of TiO2 and CdS semi-conductor photocatalysts in aqueous solution.

n-type Semiconductor	Valence band*	Conductance band*	Bad gap (eV)	Band gap (nm)
TiO_2	**+ 3.1**	**- 0.1**	**3.2**	**387**
CdS	**+2.1**	**- 0.4**	**2.5**	**496**

*(V vs.NHE)

Table 3: Initial degradation rates and degradation % of Dyes 1 and 2 using CdS/TiO_2 suspensions at pH = 7.1.

Semiconductor	Crystallite size/nm		Size Ratio R/A	% $R^{\#}$	Band gap/nm	k/min^{-1}		*D %	
						Dye1	Dye2	Dye1	Dye2
	Anatase A	Rutile R							
TiO_2	23	33.8	1.47	24.4	387	0.14	0.05	87.0	51.5
CdS(2%)/TiO_2	15	17.6	1.17	28.5	496	0.23	0.07	100	65.0

% $R^{\#}$ = [I_R/I_A] where I_R and I_A are the diffraction intensities of the (1 1 0) rutile and (1 0 1) anatase crystalline phases at 2θ = 27.58 and 25.38, respectively *Time of irradiation is 20 min.

Data of Table 3 indicate that decreasing rutile to anatase size ratio seems to play a partial role in enhancement of degradation rate and degradation % due to increasing surface area of TiO2 in the combined state with CdS. Although the increase of the percentage of rutile phase, which is photocatalytically inactive, the capability of synergistic visible light absorption due to CdS combined particles plays the major role in the catalytic efficiency enhancement as reflected in the numbers shown in Table 3.

Synergistic Photocatalytic Activity

It is well known that, for the photocatalytic oxidation (TiO_2/UV) the semiconductors absorb UV light and hydroxyl radicals are generated mainly from the absorbed H_2O and hydroxide ions. The mechanism of the TiO_2/UV degradation has been very well described in the literature using the band-gap model. It is well established that by irradiation of an aqueous TiO_2 suspension with light energy greater than the band gap energy of the semiconductor conduction band electrons and valence band holes are generated, which result in generation of different reactive species such as $O_2^{-\bullet}$ and $OH^{\bullet}$ radicals. These acts as strong oxidizing agents that can easily attack any organic molecules adsorbed on or located close to the surface of the catalyst, thus leading to their complete degradation into small inorganic species.

The new TiO_2 (R/A = 1.17, refer to Table 3) /CdS (2%, cubic) nanosized photocatalyst is prepared by simple combustion method. XRD given in Fig. 2 reveals hexagonal CdS nano particles. The TEM results in Fig. 3 confirm size reduction of TiO_2 induced by the presence of CdS, indicating that the composite is not constituted of a mere physical mixture of both components. This photocatalyst exhibits a wide absorption range (200–540 nm) in both ultraviolet and visible regions (UV–VIS region), and exhibited relatively high photocatalytic activities of 100% degradation at a rate of 0.23 min^{-1} (see Fig. 5) relative to 87% degradation at a rate of 0.014 min^{-1} for TiO_2 (R/A=1.47)/UV in case of dye 1. The maximum photo degradation efficiencies (D%) of TiO_2/CdS are 100 and 17% under UV-VIS light and visible light (410–750 nm), respectively in case of dye 1. Complete data are given in Table 3. It is worth mentioning that the more photo liability of Dy1 is most probably due to the easy cleavage of the bulky $N(CH_3)_2$ groups, which significantly depress electron delocalization leading to bond weakening.

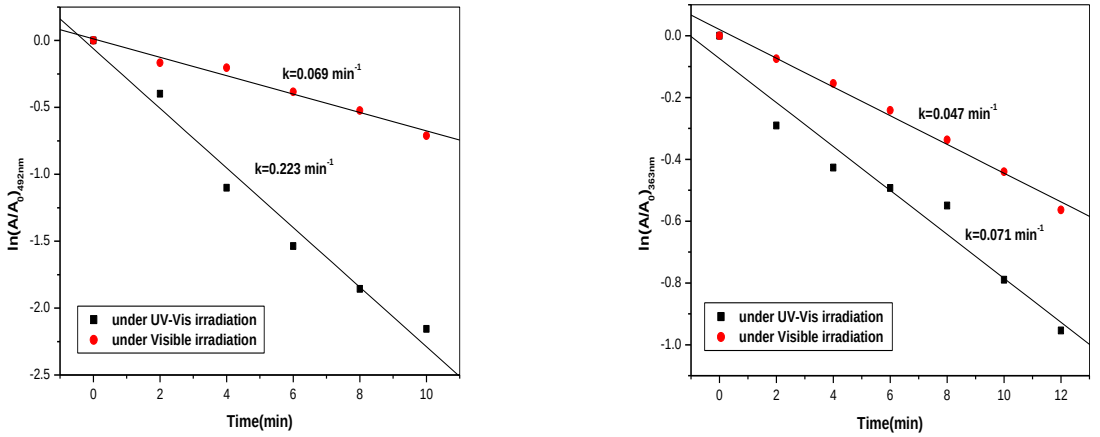

Fig 5: Comparison between the first order linear plots of decolonization of Dye 1 [2.0x10^{-5} M] a] and Dye 2 [2.0x10^{-4} M] b] by CdS/TiO_2 under UV-Vis and under visible light. ($\lambda_{analytical}$=480 nm)

Fig. 4 (b) depicts the emerged blue shift of the dye spectrum as the degradation reaction proceeds, which supports splitting of the $N(CH_3)_2$ groups leading to decolorization.

When CdS was formed by simple combustion technique and simultaneously mixed with TiO_2, a good electro-contact heterojunction was formed between TiO_2 and CdS. Under uv-visible light illumination, the electrons are excited into the CdS and TiO_2 conduction bands followed by a quick extra injection from CdS into theTiO_2 conduction band and holes are migrated from TiO_2 VB to CdS VB. The band-gap match between CdS and TiO_2 can effectively increase the photoelectron–hole separation as shown in Fig. 6[9-11,13]. Also, the formation of the heterojunctions strongly decreases the photogenerated carrier recombination. Therefore, these synergistic effects between CdS and TiO_2 should result in improving the photo conversion performance of the CdS/TiO_2.

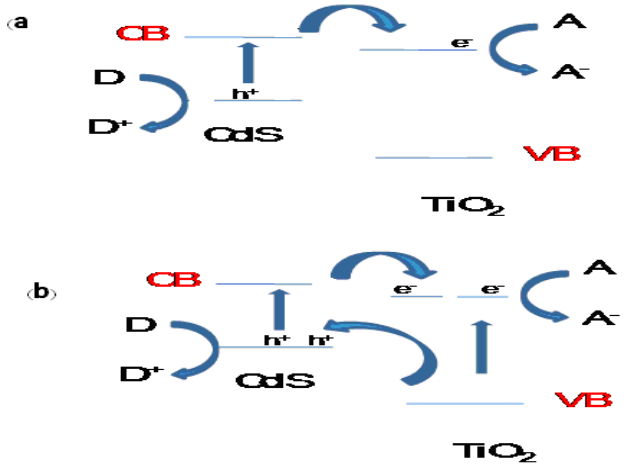

Fig. 6: (a) A sketch of an Energy level diagram illustrating the coupling of CdS/TiO2, in which electron transfer occurs from the visible light-activated CdS to the nonactivated TiO_2. The reaction CdS(e^- + h^+)–TiO_2 → CdS(h^+)–TiO_2(e^-) accounts for the synergistic effect of visible light absorption by CdS, which injects more electrons to the energetically available conduction band of the TiO_2 (b) Energy level diagram showing the coupling of CdS and TiO2, in which movement of both the electrons and holes is possible leading to synergistic e^-/h^+ production and separation.

Conclusion

The TiO_2/CdS composite material is successfully prepared by thermolysis technique. The CdS nanoparticle uniformly distribute not only on the surface of TiO_2 but also inside the TiO_2 particle, which lead to the formation of TiO_2/CdS particles with a spatial network CdS particle distribution. The results obtained from the photodegradation tests indicated that the sensibilization of narrow-band-gap CdS on broad-band-gap TiO_2 expands the photoabsorption range and makes the threshold value of the photoelectric response have an obvious red shift. Furthermore, CdS can accelerate the transfer of the photogenerated electrons and restrain the combination of carriers. Therefore, the sensibilization of CdS on TiO_2 can effectively improve the photo degradation efficiency of the TiO_2.

In our nanosized CdS coupled TiO_2 nanocrystalline system, coupling of two such semiconductor has a beneficial role in improving charge separation and extends visible light absorption at about 550 nm. The coupled catalyst exhibits high efficiency for the decomposition of dye 1 and 2 in water under Uv-visible light irradiation. Furthermore, the more photo liability of Dye1 is most probably due to the easy cleavage of the bulky $N(CH_3)_2$ groups, which significantly depress electron delocalization leading to bond weakening.

References

1) Xie Y., Chen F., He J., Zhao J., Wang H. (2000). Photoassisted degradation of dyes in the presence of Fe2O3 and H_2O_2 under visible irradiation. J Photochem Photobiol A: Chem, 136: 235e40.

2) Padoley K.V., Mudliar S.N., Pandey R.A. (2008). Heterocyclic nitrogenous pollutants in the environment and their treatment options – An overview. Bioresource Tech. 99: 4029–4043.

3) Zhang Y., Padhyay A., Sevilleja J. E., Guerrant R. L. and Geddes C. D. (2010). Interactions of Fluorophores with Iron Nanoparticles: Metal-Enhanced Fluorescence, *J. Phys. Chem*, 114: 7575–7581.

4) Ullmann's encyclopedia of industrial chemistry (2001). 6th ed. New York: Wiley-VCH;Part A27. Triarylmethane and diarylmethane dyes.

5) Faisal M, Tariq MA, Muneer M. (2007). Photocatalysed degradation of two selected dyes in UV-irradiated aqueous suspensions of titania. *Dyes Pig.* , 72:233e9.

6) Konstantinou I. K., Albanis T. A. (2004). TiO_2-assisted photocatalytic degradation of azo dyes in aqueous solution: kinetic and mechanistic investigations: a review. Appl Catal B: Environ, 49:1e14

7) Abdel-Mottaleb M. S. A. (2009). Duality of TiO_2 nanoparticles: applications in photocatalysis and dye-sensitized solar cells fabrication, *Int. J. Nanomanufacturing*, Vol. 4, Nos. 1/2/3/4.

8) Abdel-Mottaleb M. S. A., Augugliaro V. and Palmisano L. (2008). Doped TiO_2 Nanomaterials and Applications. Intern. J. Photoenergy Vol. 2008, Article ID 419096doi:10.1155/2008/419096.

9) Emeline A. V., Kuznetsov V. N., Rybchuk V. K. and Serpone N. (2008). Visible-Light-Active Titania Photocatalysts: The Case of N-Doped TiO_2s—Properties and Some Fundamental Issues, *Intern. J. Photoenergy* Vol. 2008, Article ID 258394, doi:10.1155/2008/258394.

10) Yu Y., Ding Y., Zuo S. and Liu J. (2011). Photocatalytic Activity of Nanosized Cadmium Sulfides Synthesized by Complex Compound Thermolysis, Vol. 2011, Article ID 762929,doi:10.1155/2011/762929.

11) Kim D. J., Yu Y.-M., Lee J. W., and Choi Y. D. 2008). "Investigation of energy band gap and optical properties of cubic CdS epilayers,*" Appl. Surf. Sci.,* 254(**22**): 7522–7526.

12) Lewandowxki M., Ollis D. F. (2004). Semiconductor photochemistry and Photophysics, in: V. Ramamurthy, K.S. Schanke (Eds.), Basel, New York, p. 249.

13) Didier R. (2007). Photosensitization of TiO_2 by MxOy and MxSy nanoparticles. *for, Catal. Today,* 122: 20–26.